



CHORUS

This is the accepted manuscript made available via CHORUS. The article has been published as:

Magnetic and structural properties of single-crystalline $\text{Er}_{5}\text{Si}_{4}$

Ya. Mudryk, Niraj K. Singh, V. K. Pecharsky, D. L. Schlagel, T. A. Lograsso, and K. A. Gschneidner, Jr.

Phys. Rev. B **85**, 094432 — Published 29 March 2012

DOI: [10.1103/PhysRevB.85.094432](https://doi.org/10.1103/PhysRevB.85.094432)

Magnetic and structural properties of single crystalline Er₅Si₄

Ya. Mudryk,^{1,*} Niraj K. Singh,¹ V.K. Pecharsky,^{1,2} D.L. Schlagel,¹

T.A. Lograsso,¹ and K.A. Gschneidner, Jr.^{1,2}

¹The Ames Laboratory of the US DOE, Iowa State University, Ames, IA 50011-3020, U.S.A. and

²Department of Materials Science and Engineering, Iowa State University, Ames, IA 50011-2300,

U.S.A.

PACS: 61.50.Ks, 75.30.Gw, 75.80.+q, 81.30.Hd

Abstract

The magnetization of the oriented Er₅Si₄ single crystal, measured along the three principal crystallographic directions reveals strong magnetocrystalline anisotropy. The *b*-axis is the easy magnetization direction. The possible presence of the crystal field effect and the non-collinear alignment of magnetic moments result in a lower than gJ magnetization along all crystallographic directions even in 70 kOe applied magnetic field, with the lowest moment ($4.22 \mu_B/\text{Er}^{3+}$) recorded along the *a* axis. The magnetization measurements show that even in the true paramagnetic state there is a weak magnetic field dependence of the structural-only transition when the field is applied along the *a* and *c* axes but this transition is magnetic field independent along the *b*-axis in fields of 70 kOe or less. The temperature and magnetic field dependent x-ray powder diffraction study of the powdered single crystal confirms the temperature driven structural orthorhombic – monoclinic transition in the paramagnetic state and the low temperature magnetic field driven monoclinic – orthorhombic transition in the magnetically ordered state. The x-ray powder diffraction indicates that the high temperature transition is magnetic field

independent below 40 kOe in a polycrystalline sample while the low temperature transition requires high magnetic field for its completion.

* corresponding author: slavkomk@ameslab.gov

Introduction

The Er_5Si_4 intermetallic compound was discovered by Smith *et al.*^{1,2} as one of several other R_5T_4 compounds, where R = rare earth element, and T = Si, Ge. The Er_5Si_4 compound was reported to crystallize with the Sm_5Ge_4 -type³ orthorhombic crystal structure. Basic magnetic properties of R_5T_4 compounds were measured for R = Gd, Tb, Dy, Ho, and Er,⁴ and it was found that the silicides order ferromagnetically (Gd_5Si_4 at 336 K), whereas the germanides order antiferromagnetically at much lower temperatures. The Er_5Si_4 was reported to order ferromagnetically at 25 K.⁴ According to the Er-Si phase diagram,⁵ Er_5Si_4 forms peritectically from liquid and Er_5Si_3 at 1875 °C.

Interest in the R_5T_4 compounds⁶ was rekindled in 1997, when the giant magnetocaloric effect was reported in the $\text{Gd}_5\text{Si}_2\text{Ge}_2$ compound and other members of the $\text{Gd}_5\text{Si}_x\text{Ge}_{4-x}$ family of materials.^{7,8} Since then, there has been a growing interest in the R_5T_4 compounds, more specifically, in the intricate relationships between their crystal structures and physical properties.⁹⁻¹⁷ While most of these studies were focused on the Gd-based R_5T_4 systems, the uniqueness of Er_5Si_4 , i.e. a clear decoupling of structural and magnetic transitions,^{6,18,19} makes it an interesting system to study. Another interesting feature, which distinguishes Er_5Si_4 among other members of the R_5T_4 family, is a presence of structural transformation in a binary silicide (T is Si), but not in a pseudo-binary germanide-silicide (T is $\text{Si}_x\text{Ge}_{1-x}$) phase.^{18,19}

At room temperature Er_5Si_4 adopts the Gd_5Si_4 -type (O-I) structure,¹⁸ and not the Sm_5Ge_4 -type (O-II) as was originally reported.³ The difference between these structure types, which adopt the same space group symmetry ($Pnma$) and have similar lattice parameters,¹⁴ is in the T - T bonding, commonly known

in the literature as the “interslab” bonding. These two structure types, as well as the related monoclinic $\text{Gd}_5\text{Si}_2\text{Ge}_2$ ^{20,21} and $\text{M}\beta\text{-Ho}_5\text{Ge}_4$ ²² types, and the orthorhombic $\text{Tm}_5\text{Sb}_2\text{Si}_2$ ²³ type structures can be represented as different stacking of quasi-two-dimensional atomic blocks or layers, sometimes also called slabs.^{6,24} The blocks are stacked along the longest unit-cell dimension, which is the b axis. The interatomic distances between the T – T atoms from neighboring layers vary in these structures from ~ 2.6 Å (bonding) to ~ 4.2 Å (no bonding). In the Gd_5Si_4 -type structure, which is the room-temperature polymorph for the Er_5Si_4 , the partially covalent T – T bonds exist between all of the slabs, while in the $\text{Gd}_5\text{Si}_2\text{Ge}_2$ -type structure (M),²⁴ which is the low-temperature form of Er_5Si_4 ,^{18,19} one half of these bonds are much longer, and therefore, weaker. The lattice is monoclinically distorted, and microscopic twinning has been observed in Er_5Si_4 single crystal.¹⁹ For a phase to adopt the Sm_5Ge_4 -type of structure (O-II), all of the interslab T – T bonds must be broken,²⁴ which was not observed in Er_5Si_4 .

Recent experimental results obtained at various pressures, temperatures, and applied magnetic fields^{18,19,25-30} showed that in Er_5Si_4 the orthorhombic (O-I) \leftrightarrow monoclinic (M) structural transition takes place at about $T_s = 200$ K on cooling, and contrary to most of the R_5T_4 systems, where structural and magnetic transitions are either concomitant or close to one another on the temperature scale,⁶ the magnetic ordering transition occurs here at a much lower temperature ($T_{\text{order.}} = 30$ K).^{25,30} The first-order structural only transformation manifests as a broad peak on the heat capacity data.³⁰ Surprisingly, the transformation at 200 K in the polycrystalline sample weakly depends on the applied magnetic field ($H = 40$ kOe and higher), despite of the paramagnetism of both phases which are involved in the transition.^{30,31}

In the magnetically ordered state below 30 K, Er_5Si_4 undergoes an incomplete magnetic field induced M FM \leftrightarrow O-I FM transformation (61 vol.% of the O-I phase is observed at $T = 2$ K, and $H = 50$ kOe).²⁷ The nature of this transformation is quite unique for the R_5T_4 systems because in this field-induced structural transition the magnetic ground state of both phases is essentially the same, while in other R_5T_4 systems the field-driven structural transitions are either paramagnetic (PM) \leftrightarrow FM ($\text{Gd}_5\text{Si}_{1.8}\text{Ge}_{2.2}$)⁹ or antiferromagnetic (AFM) \leftrightarrow FM (Gd_5Ge_4).³²

The magnetic structure of Er_5Si_4 compound was first studied using neutron diffraction by Cadogan *et al.*,³³ and the coexistence of both ferromagnetic and antiferromagnetic ordering in this compound was reported below 32 K. The Sm_5Ge_4 -type structure was reported at all temperatures but with lattice parameters typical for the Gd_5Si_4 -type structure. Recent neutron diffraction experiments performed in zero magnetic field^{25,27} reported the monoclinic crystal structure for the magnetically ordered phase in agreement with x-ray diffraction studies.^{18,19} The canted magnetic structure of Er_5Si_4 has an easy magnetization direction along the b -axis, and a strong AFM component within the ac plane. Interestingly, the magnetic structure of the orthorhombic Er_5Si_4 ^{27,33} is similar to the magnetic structure of the monoclinic Er_5Si_4 ,^{25,27} i.e. both polymorphs show the same easy magnetization b -axis and the same ac plane for AFM interactions. The high-field O-I phase has nearly collinear alignment of magnetic moments along the easy magnetization axis.²⁷

Another important property recently discovered in Er_5Si_4 is extraordinary sensitivity of the crystal lattice to the applied hydrostatic pressure.^{26,28} The temperature of the O-I to M transformation in the paramagnetic state was found to change with an exceptionally high rate of $dT_s/dP = -30$ K/kbar. Application of hydrostatic pressure also shifts the temperature of the low-temperature M to O-I

transformation (T_t) at much lower but still significant $dT_t/dP = 6$ K/kbar rate. Above 6 kbar both transitions merge and a stable O-I phase exists throughout the whole examined temperature range (2 – 300 K).²⁶ The constructed P-T phase diagram^{26,28} shows that four different transitions occur in the system: O-I-PM \leftrightarrow M-PM, O-I-FM \leftrightarrow M-FM, M-FM \leftrightarrow M-PM, and O-I-FM \leftrightarrow O-I-PM – a unique feature among all other R_5T_4 systems studied to date. The applied pressure also enhances FM interactions in the Er_5Si_4 due to the formation of the O-I phase with more collinearly aligned moments.²⁶⁻²⁹ It also leads to the enhancement of the magnetocaloric effect in Er_5Si_4 .²⁹

This interesting behavior of the Er_5Si_4 compound warrants further investigation of its crystallography and magnetism using a single crystal, since all previous studies were performed using polycrystalline materials. It would be particularly interesting to establish whether the magnetic field induced shift of the temperature of the transition at ~ 200 K is anisotropic and how this shift relates with the magnetic properties of Er_5Si_4 along different crystallographic directions. This work presents a detailed study of the magnetic properties of Er_5Si_4 along three major crystallographic directions combined with temperature- and magnetic field dependent high-resolution x-ray powder diffraction, which directly provides information about the transformations of the crystal structure of the investigated material.

Experiment

The sample used in the investigation was extracted from a large single crystal, grown by a modified Bridgman method³⁴ from stoichiometric amounts of high purity erbium (99.99 wt.% or 99.9 at.% purity with respect to all other elements in the Periodic Table; main impurities were O – 397 at. ppm and C – 278 at. ppm)³⁵ and silicon (purchased from Alfa Aesar, 99.9995 wt.% pure). Some tungsten from the

crucible has been detected as a minor impurity in the x-ray powder diffraction pattern collected after grinding a small portion of this Bridgman-grown single crystal; very weak Bragg peaks of Cu from a sample holder contamination of the surface during sample preparation³⁷ are seen in the x-ray diffraction patterns as well (Fig. 1a). We note that while the W contamination exists as small dendrites formed during crystal growth, the Cu contamination is completely extrinsic to the material and was only present in the specimen prepared for x-ray powder diffraction examination. Neither the minor W impurity nor the minor Cu surface contamination has any noticeable effect on both structural and magnetic properties of the material reported here.

The magnetic measurements were performed on the oriented single crystalline parallelepiped with dimensions of $0.50 \times 0.83 \times 1.00$ mm³. The misalignment between the crystallographic directions and the magnetic field vector was less than 5°. The Quantum Design superconducting quantum interference device (SQUID) magnetometer (model MPMS XL-7) was used for magnetization and magnetic susceptibility measurements at temperatures between 1.8 K and 300 K, and in magnetic fields up to 70 kOe. $M(H)$ data presented in the manuscript and $HM^1(T)$ data that were used in Curie-Weiss fits were corrected for demagnetization as described by Chen *et al.*³⁶ The fields reported in $M(T)$ and $HM^1(T)$ plots are applied dc magnetic fields.

All x-ray measurements were performed by using the Rigaku TTRAX diffractometer (Bragg-Brentano geometry, Mo K_α radiation) equipped with a continuous flow helium cryostat, and a split-coil superconducting magnet.³⁷ The 2θ range of the measured Bragg angles for the regular x-ray patterns was from 9 to 49 deg. 2θ ($\Delta 2\theta = 0.01^\circ$). In order to quickly determine the concentration of phases during the structural transition as a function of temperature, short scans were performed in the range of

9 - 27 deg. 2θ . Temperature range of data collection was from 5 to 300 K. Magnetic fields applied were from 0 to 40 kOe.

The collected x-ray powder diffraction patterns were analyzed using Rietveld refinement program LHPM Rietica.³⁸ The coordinates of individual atoms were refined if the amount of the corresponding phase was 20 mol.% or more. The isotropic thermal displacement parameters of all atoms in each phase were assumed to be the same, in effect, employing the overall isotropic thermal displacement approximation. The final profile residuals (R_p) were lower than 10 %, and the derived Bragg residuals (R_B) were less than 6 % for any polymorphic form of Er_5Si_4 . The negligible difference in the linear absorption coefficients of the two Er_5Si_4 polymorphs, and low preferred orientation, achieved by careful specimen preparation,³⁷ makes the Rietveld-based quantitative phase analyses quite accurate and reliable. All things considered, the phase contents were determined with ~ 1 mol.% accuracy, which is derived from least squares standard deviations of phase scale factors.

Results

Magnetic measurements

The magnetization measured as a function of temperature (Fig. 2) shows that at 30 K in magnetic fields below 30 kOe the Er_5Si_4 undergoes an AFM-like transition along the a - and c -axes but the transition along the b -axis is typical for a ferromagnet. At fields higher than 30 kOe the Er_5Si_4 becomes FM-like in all directions, but the net magnetization is lower along the a -axis compared with the same along the b and c axes (Fig. 2). The high-temperature structural (~ 200 K) transition is clearly seen on HM^1 vs T

plots, which are shown for 1 kOe dc field (Fig. 3). The transition is broad and its temperature limits are not well-defined. The deviations from linearity in the $HM^1(T)$ lines are nearly identical for the a - and c -directions but are a few degrees higher for the b -axis. Taking the discontinuity (peak) temperature of the $d(HM^1)/dT$ curves as the transition temperature, one finds that it decreases nearly linearly with the applied magnetic field (Fig. 4) along a - (-0.026 K/kOe) and c -axes (-0.043 K/kOe) while it is field independent when H is parallel to the b -axis. The lowering of the transition temperature in high magnetic field in the ac -plane agrees, in general, with the heat capacity results obtained on a polycrystalline Er_5Si_4 sample.³⁰ The absence of this effect with magnetic field along the easy magnetization axis may explain why it is also harder to notice such field dependence in polycrystalline samples (also see x-ray powder diffraction measurements, below). The paramagnetic Weiss constants (θ_p) are different for the three main crystallographic directions indicating magnetocrystalline anisotropy in both the O-I and M phases (Fig. 3). The strongest ferromagnetic interactions ($\theta_p = 44.8$ K) are recorded along the b -axis for the O-I phase, which has the nearly collinear alignment of magnetic moments in that direction in the magnetically ordered state.²⁷

The magnetization at 5 K as a function of applied magnetic field (Fig. 5) is strongly anisotropic, in full agreement with the microscopic magnetic structure obtained by the neutron diffraction studies.^{25,27,33} The b -axis is the easy magnetization direction. Application and removal of magnetic field at 5 K leads to multiple metamagnetic-like transitions along the c -axis. For the a -axis, a change of slope at 30 kOe in the $M(H)$ curve recorded at 5 K is the indication of a field-induced spin reorientation. The c -axis is the only axis that exhibits noticeable hysteretic features on the $M(H)$ curves at 5 K (Fig. 5) and the multistep behavior, which, however, changes to a one step spin reorientation at high temperatures. The three steps on the $M(H)$ c -axis data correspond to the spin reorientation of magnetic moments of three kinds of Er

atoms in the monoclinic structure. As follows from neutron scattering data of both the monoclinic Er_5Si_4 ^{25,27} and the orthorhombic Er_5Si_4 ³³ it is expected that each pair of the four-fold Er positions in the M structure formed from the splitting of the eight-fold Er positions of the O-I structure behaves as one group, thus leading to only three independent Er sites, even though all five four-fold Er sites in the monoclinic Er_5Si_4 structure are formally independent. Of these sites, two contain 8 Er atoms each and one accommodates 4 Er atoms, which approximately corresponds to the magnitudes of the three steps observed in Fig. 5 for the *c*-axis. There is no hysteresis or spin reorientation transition along the *b* direction reflecting the fact that the magnetic moments are already aligned in that direction in zero field [both in the O-I and M phases]. We note, however, that none of the $M(H)$ curves exhibit a single and clear metamagnetic-like transition that can be associated with the M – O-I structural transformation. This is understood considering that microscopic magnetism of the O-I and M phases in Er_5Si_4 is similar,^{25,27,33} while it is different in other R_5T_4 systems (i.e. in $\text{Gd}_5\text{Si}_2\text{Ge}_2$).^{9,24,39,40} The magnetic field in Er_5Si_4 , as a thermodynamic variable, is therefore, not a strong driving force triggering the structural transition compared to temperature or pressure, contrary to that observed in the Gd_5T_4 systems.⁴¹ Thus, the sluggish development of the magnetostructural transition in Er_5Si_4 is masked by much sharper spin-reorientation transitions.

The magnetization in 70 kOe applied magnetic field is $4.22 \mu_{\text{B}}/\text{Er}^{3+}$ for the *a*-axis, $6.50 \mu_{\text{B}}/\text{Er}^{3+}$ for the *c*-axis, and $6.86 \mu_{\text{B}}/\text{Er}^{3+}$ for the *b*-axis, all of which are significantly lower than the theoretical gJ value of $9 \mu_{\text{B}}$. According to the magnetic structure,^{25,27} the magnetic moments are not collinear in Er_5Si_4 compound along the *a*-axis, which is confirmed by the present $M(H)$ measurements (Fig. 5). The non-collinearity in 70 kOe field is also possible along *c*- and even *b*-axes, but strong crystal field effects should also be considered as a reason for the low experimental saturation moments in Er_5Si_4 . The

magnetocaloric effect (magnetic entropy change, ΔS_M), which was calculated from the $M(H)$ data, is the largest (-20 J/Kg K at 30 K) for the b -axis, moderate (-12 J/Kg K at 32 K) for the c -axis, and smallest (-8 J/Kg K at 32 K) for the a -axis ($\Delta H = 0-50$ kOe). Consequently, for the ideal (randomly oriented) polycrystalline sample the average ΔS_M should be -13.3 J/Kg K, which agrees well with the $\Delta S_M = -14.9$ J/Kg K value previously reported for the polycrystalline Er_5Si_4 .²⁹

The ac magnetic susceptibility indicates an ordering transition at 30 K for all directions (Fig. 6). The imaginary part of the magnetic susceptibility (inset in Fig. 6) is different along the principal crystal axes. Since a non-zero value of χ'' reflects energy loss due to domain wall motion, the presence of the distinct peak in the χ'' data measured along the b -direction indicates that a small magnetic field applied along the b -axis can alter the arrangement of magnetic domains. This is consistent with the dc $M(H)$ data, which indicate the b -direction as the easy axis. The spin-reorientation transition reported in the literature around 15 K^{11,25} is seen along the c -axis in both magnetization (Fig. 2) and susceptibility (Fig. 6) data.

X-ray powder diffraction

A broad structural O-I- $\text{Er}_5\text{Si}_4 \leftrightarrow$ M- Er_5Si_4 transition occurs between 220 K and 180 K on cooling and between 200 K and 240 K on heating (Fig. 7), in agreement with the transformation temperatures from Ref. 30, and in partial agreement with single crystal magnetization data (Fig. 3). Both the transition range and thermal hysteresis are wider compared to the single crystal studies, as expected for polycrystalline samples in general. Surprisingly, about 30 mol.% of M- Er_5Si_4 phase was observed at room temperature according to the Rietveld refinement results (Fig. 1a). Further experiments show that the amount of the monoclinic Er_5Si_4 phase at room temperature is proportional to the time of grinding

the sample into a powder and it does not matter whether the sample was ground in open air or in an Ar-filled glove box, thus ruling out the potential effect of oxygen contamination. A mechanism of such change is currently under investigation. A detectable amount of the O-I phase (~7 mol.%) is observed at low temperatures (the pattern collected at 50 K is shown in Fig. 1b). The lattice parameters and unit-cell volume behavior is characterized by two anomalies, a strong one around the structural transition (Fig. 8), and another, much weaker increase in the a lattice parameter observed at 30 K (Fig. 9).

High resolution of x-ray powder diffraction data allows the investigation of the lattice parameters of a minority phase as well. Thus, the lattice parameters behavior of Er_5Si_4 during the O-I \leftrightarrow M transformation can be analyzed from two different aspects. First, there is a substantial difference in the lattice parameters between O-I- Er_5Si_4 and M- Er_5Si_4 structures. In principle, despite the reverse temperature order, the behavior of lattice parameters follows the orthorhombic – monoclinic transition in $\text{Gd}_5\text{Si}_2\text{Ge}_2$:^{9,24,41} a large change in the a parameter ($\Delta a/a = -0.99\%$) is accompanied by a smaller change in the c parameter with an opposite sign ($\Delta c/c = 0.40\%$), and by an even smaller change in the b parameter ($\Delta b/b = -0.23\%$) (Fig. 8). The resulting unit cell volume change is quite substantial ($\Delta V/V = -0.68\%$). The values of the observed changes are in good agreement with those obtained in the neutron diffraction experiment.²⁵ Second, the behavior of the lattice parameters of each phase below and above the transition follows a normal thermal expansion behavior. The strong deviations in lattice parameters near the structural transition temperature were reported in the Er_5Si_4 single crystal x-ray diffraction study,¹⁹ and were explained by possible intermediate states, which occur due to a gradual distortion of the M phase over an extended period of time. However, in our x-ray powder diffraction data these anomalies are not observed (Fig. 8). It is possible that the much broader transition of the polycrystalline sample has an averaging effect on the determined lattice parameters thus masking the phenomena

observed in single crystals. On the other hand, lattice parameters determined from single crystal x-ray diffraction data are much less accurate compared to the same determined from powder diffraction data, and therefore, anomalies reported in Ref. 19 need further confirmation.

The investigation of the influence of the applied magnetic field on the lattice parameters was performed at low temperatures (at $T = 7, 15$ and 25 K) and near the first-order structural transformation. The temperature dependence of the phase composition obtained at 40 kOe fully matches the curve obtained at 0 kOe (Fig. 7), so no influence of the 40 kOe magnetic field on the $M\text{-Er}_5\text{Si}_4 - \text{O-I-Er}_5\text{Si}_4$ first-order structural transformation in the polycrystalline sample was observed, in agreement with the heat capacity data,³⁰ where 40 kOe field was reported to be too low to induce a shift in the transition temperature. Both the different nature of the samples (polycrystalline vs. single-crystalline) and the larger temperature steps (0.5 K minimum) of the x-ray measurement probably mask the field dependence of the structural transition clearly observed in the single crystal magnetization data (Fig. 3).

Below 30 K the concentration of the orthorhombic phase increases slightly with increasing magnetic field. The isothermal experiments were carried out at $7, 15,$ and 25 K (Fig. 10). At $H = 40$ kOe and $T = 7$ K the concentration of the $\text{O-I-Er}_5\text{Si}_4$ phase is ~ 15 mol.%, which is about twice that of the observed concentration of this phase at and above 25 K (7 mol.%). Thus, the experiment confirms the literature report²⁷ that the increase of the high-temperature O-I phase content below the magnetic ordering temperature ($T_{\text{order.}} = 30$ K) is real, and that the structural transformation can be driven by both a temperature decrease and an increase of the applied magnetic field. In stronger magnetic fields the amount of $\text{O-I-Er}_5\text{Si}_4$ would be higher.²⁷ The lattice parameters and the unit-cell volume of the monoclinic phase change slightly in applied magnetic fields at and below 40 kOe (Figure 11). The

magnetic field induces the stronger expansion of the crystal lattice for the a - and c -axes compared to the b -axis.

Discussion

The Er_5Si_4 compound has similarities with other studied members of the R_5T_4 series of materials,⁶ but it also has some unique structural and magnetic properties. The high-temperature (or room-temperature) polymorphic modification of Er_5Si_4 belongs to the orthorhombic Gd_5Si_4 -type structure, but below ~ 200 - 220 K it adopts the monoclinic $\text{Gd}_5\text{Si}_2\text{Ge}_2$ -type structure. Unlike the well-studied $\text{Gd}_5(\text{Si}_x\text{Ge}_{1-x})_4$ system, where the Gd_5Si_4 -type – $\text{Gd}_5\text{Si}_2\text{Ge}_2$ -type structural transformation is strongly coupled with magnetic transformation,^{6,9,14,24} Er_5Si_4 shows a substantial decoupling between the temperatures of the magnetic ordering ($T_{\text{order.}} = 30$ K) and the structural transformation ($T_s = 200$ K).^{18,19,30} At the same time there is a substantial interaction between the crystal and magnetic sublattices in this compound,²⁷ and applied magnetic field increases net magnetic moment in this compound through the modification of its crystal structure below 30 K when the ground state is essentially the same.

While the structural transition around 200 K is obvious in many Er_5Si_4 samples,^{18,19,27} and is confirmed by the present study, it was not observed in some other works.³³ Impurities are known to stabilize certain polymorphic modifications in R_5T_4 systems,⁴² and this is the likely scenario in Er_5Si_4 , which is confirmed by the fact that samples made from high purity Er always show both structural modifications. Another possibility involves stresses present in the sample taking into account the extraordinary sensitivity of the ~ 200 K transformation to pressure.²⁶ Such stresses may be a result of a sample preparation (i.e. thermal and/or mechanical treatment). Indirect evidence of the influence of mechanical

deformation on the concentration of the M-Er₅Si₄ phase present was noted above, where we found that the concentration of this phase at room temperature increases as a function of grinding time during preparation of the specimen for the powder diffraction experiment.

The magneto-structural coupling is strong below 30 K when magnetic interactions start to play a significant role. The magnetic field induced transition from the monoclinic to the orthorhombic phase in Er₅Si₄ was observed by linear thermal expansion measurements and neutron diffraction experiments,²⁷ and is supported by the present study. But Er₅Si₄ is more sensitive to an applied pressure than to an applied magnetic field²⁶⁻²⁸ when compared to the earlier studied Gd₅(Si_xGe_{1-x})₄ compounds, i.e. Gd₅Si_{1.8}Ge_{2.2}⁹ or Gd₅Si₂Ge₂,⁴³ which required lower critical magnetic fields to trigger and complete M to O-I transition, but corresponding T_C is less sensitive to the applied hydrostatic pressure. The fact that the O-I-Er₅Si₄ structure is stable over the whole temperature range (0 to 300 K) at 6 kbar or higher^{26,28} also supports this suggestion.

Surprisingly, the high temperature M-PM to O-I-PM transition also shows weak magnetostructural coupling as noted in the heat capacity³⁰ and single crystal magnetization measurements (Fig. 4). It is quite unique in the paramagnetic state, where magnetic moments are non-interacting and their orientation is expected to be random that such a behavior is found; however, it is typical for alloys that exhibit long range magnetic order. This coupling is also related to the magnetic structure of the compound in the ordered state:^{25,27} apparently, it is easier to rotate magnetic domains along the *b*-direction in the ordered state than along *a*- or *c*- direction. In the paramagnetic state, the non-interacting magnetic moments respond to the external magnetic field *H* by forming preferred orientation direction of the magnetic moments in the direction of the field. If there is a correlation between the magnetic

moments and magnetic domains in Er_5Si_4 , the field-induced rotation of the moments along the a - and c -axes may induce greater strain than along the b -axis. Indeed, the magnetostriction measured using the field dependent x-ray powder diffraction at 7 K indicates that the crystal lattice expands in a field applied along the a - and c -directions, but not as much along the b -direction (Figure 11). The θ_p constants vary significantly along the three main crystallographic directions indicating that magnetocrystalline anisotropy is present in the paramagnetic state of Er_5Si_4 (Fig. 3). Given the extraordinary sensitivity to pressure in Er_5Si_4 , one may speculate that it is the field induced preferred orientation of non-interacting magnetic moments and the resulting weak magnetostriction in the case of $H\uparrow a$ or $H\uparrow c$ that causes the shift of the structural transition temperature.

While the origin of the magnetocrystalline anisotropy in Er_5Si_4 is not the main subject of this manuscript, and requires further theoretical and experimental investigation, it is possible to make a few remarks based on the current body of knowledge about this and other R_5T_4 systems. First, the crystal structure of Er_5Si_4 is quite complex and contains several crystallographically independent rare earth positions allowing various magnetic structures with different net magnetic moments along the three major crystallographic directions. The most energetically stable magnetic structure apparently arises from the competition between complex electronic band structure configurations coming from the RKKY-type indirect exchange interactions. As it was shown in the $\text{Gd}_5\text{Si}_x\text{Ge}_{4-x}$ system, the hybridization between $4p$ orbitals of non-magnetic Ge (and/or $3p$ orbitals of non-magnetic Si), and $5d$ orbitals of Gd plays a critical role in mediating long-range ferromagnetic interactions between $4f$ orbitals of the rare earth atoms.⁴⁴ The non-magnetic T elements become polarized through the p - d hybridization. However, the main contribution to the band structure generally comes from the $4f$ - $5d$ spin mixing of rare earth atoms and the fact that the $5d$ magnetic moments that may be as high as $\sim 0.5 \mu_B/\text{Gd}$ as calculated

from first principles and observed experimentally in several $\text{Gd}_5\text{Si}_x\text{Ge}_{4-x}$ compounds.^{45,46} While these moments are about an order of magnitude lower than the localized $4f$ moments, it is known that their values strongly correlate with the basic magnetism of R_5T_4 compounds, i.e. higher $5d$ moments support FM interactions, while lower $5d$ moments are typical for the AFM ground states.⁴⁶ One can assume that this picture is still valid for Er_5Si_4 , even though additional verification would be useful. In Er_5Si_4 , however, the interactions are more complicated because in addition to the crystallographic anisotropy of R_5T_4 structures the intrinsic single-ion anisotropy of Er starts to play a significant role. It is also reasonable to assume that the existing polarization of the conduction bands and orbital moment contribution from $4f$ electrons⁴⁷ affects spin-orbit coupling of the system leading to an energy landscape that favors magnetic anisotropy and non-collinearity of the spins.

Conclusions

The Er_5Si_4 compound shows different magnetic behavior along different crystallographic directions as expected from its complex magnetic structure. The b -axis is the easy magnetization direction, while it is hard to align magnetic moments in the a -direction even at 70 kOe. Both crystal field effects and the non-collinear magnetic structure may result in magnetic moments, which are less than the theoretical value of $gJ = 9 \mu_B/\text{Er}^{3+}$ in Er_5Si_4 . The high temperature PM O-I \leftrightarrow PM M transformation in Er_5Si_4 is suppressed by a few degrees when the magnetic field is applied along the a or c axes of the single crystal but no such change is observed along the b -axis. Taking into account the extraordinary sensitivity to pressure in Er_5Si_4 , and the presence of the magnetocrystalline anisotropy in the paramagnetic state of Er_5Si_4 , we suggest that the field induced preferred orientation of non-interacting magnetic moments and weak but non-negligible magnetostriction in the case of $H \uparrow a$ or $H \uparrow c$ causes the shift of the structural

transition temperature. The temperature dependent x-ray powder diffraction investigation of Er_5Si_4 confirms the presence of the first-order structural transition $\text{O-I-Er}_5\text{Si}_4 \leftrightarrow \text{M-Er}_5\text{Si}_4$ at ~ 200 K. However, the x-ray studies show that the high temperature structural transformation in polycrystalline samples is not influenced by applied magnetic fields up to 40 kOe. At the same time, the amount of the orthorhombic phase increases below the magnetic ordering temperature of 30 K when a magnetic field is applied.

The magnetic structures of monoclinic and orthorhombic phases are quite similar, and, therefore, magnetic field is a weak thermodynamic stimulus in Er_5Si_4 . The magnetostriction is small along the a - and c -axes of the Er_5Si_4 crystal structure in the ordered state, and it is even smaller along the b -axis. During the first-order transformation, however, the spontaneous volume change is significant ($\Delta V/V = -0.68\%$) due to a substantial difference in the lattice parameters of the two polymorphs.

Acknowledgements

Work at Ames Laboratory is supported by the Office of Basic Energy Sciences, Materials Sciences Division of the Office of Science, U.S. Department of Energy. The Ames Laboratory is operated by Iowa State University of Science and Technology for the U.S. Department of Energy under contract No. DE-AC02-07CH11358.

References

- ¹ G. S. Smith, A. G. Tharp, and Q. Johnson, *Nature* **210**, 1148 (1966).
- ² G. S. Smith, A. G. Tharp, and Q. Johnson, *Acta Cryst.* **22**, 940 (1967).
- ³ G. S. Smith, Q. Johnson, and A. G. Tharp, *Acta Cryst.* **22**, 269 (1967).
- ⁴ F. Holtzberg, R. J. Gambino, and T. R. McGuire, *J. Phys. Chem. Solids* **28**, 2283 (1967).
- ⁵ S. P. Luzan, V. E. Listovnichii, Yu. I. Buyanov, and P. S. Martsenyuk, *J. Alloys Compd.* **239**, 77 (1996).
- ⁶ V. K. Pecharsky and K. A. Gschneidner, Jr., *Pure Appl. Chem.* **79**, 1383 (2007), and references therein.
- ⁷ V. K. Pecharsky and K. A. Gschneidner, Jr., *Phys. Rev. Lett.* **78**, 4494 (1997).
- ⁸ V. K. Pecharsky and K. A. Gschneidner, Jr., *Appl. Phys. Lett.* **70**, 3299 (1997).
- ⁹ L. Morellon, P. A. Algarabel, M. R. Ibarra, J. Blasco, B. Garcia-Landa, Z. Arnold, and F. Albertini, *Phys. Rev. B* **58**, R14721 (1998).
- ¹⁰ L. Morellon, C. Magen, P. A. Algarabel, M. R. Ibarra, and C. Ritter, *Appl. Phys. Lett.* **79**, 1318 (2001).
- ¹¹ J. M. Cadogan, D. H. Ryan, Z. Altounian, B. H. Wang, and I. P. Swainson, *J. Phys.: Condens. Matter* **14**, 7191 (2002).
- ¹² R. Cerny and K. Alami-Yadri, *Acta Cryst. E* **E59**, i1 (2003).
- ¹³ V. V. Ivchenko, V. K. Pecharsky, and K. A. Gschneidner, Jr., *Adv. Cryog. Eng.* **46A**, 405 (2000).
- ¹⁴ A. O. Pecharsky, K. A. Gschneidner, Jr., V. K. Pecharsky, and C. E. Schindler, *J. Alloys Compd.* **338**, 126 (2002).
- ¹⁵ C. Ritter, L. Morellon, P. A. Algarabel, C. Magen, and M. R. Ibarra, *Phys. Rev. B* **65**, 094405 (2002).

-
- ¹⁶ H. F. Yang, G. H. Rao, G. Y. Liu, Z. W. Ouyang, W. F. Liu, X. M. Feng, W. G. Chu, and J. K. Liang, *J. Alloys Compd.* **348**, 150 (2003).
- ¹⁷ J. D. Moore, K. Morrison, G. K. Perkins, D. L. Schlagel, T. A. Lograsso, K. A. Gschneidner, Jr., V. K. Pecharsky, and L. F. Cohen, *Adv. Mater.* **21**, 3780 (2009).
- ¹⁸ V. K. Pecharsky, A. O. Pecharsky, Y. Mozharivskyj, K. A. Gschneidner, Jr., and G. J. Miller, *Phys. Rev. Lett.* **91**, 207205 (2003).
- ¹⁹ Y. Mozharivskyj, A. O. Pecharsky, V. K. Pecharsky, G. J. Miller, and K. A. Gschneidner, Jr., *Phys. Rev. B* **69**, 144102 (2004).
- ²⁰ V. K. Pecharsky and K. A. Gschneidner, Jr., *J. Alloys Compd.* **260**, 98 (1997).
- ²¹ W. Choe, V. K. Pecharsky, A. O. Pecharsky, K. A. Gschneidner, Jr., V. G. Young, and G. J. Miller, *Phys. Rev. Lett.* **84**, 4617 (2000).
- ²² N. K. Singh, Durga Paudyal, Ya. Mudryk, V. K. Pecharsky, and K. A. Gschneidner, Jr., *Phys. Rev. B* **79**, 094115 (2009).
- ²³ A. Yu. Kozlov, V. V. Pavlyuk, and V. M. Davydov, *Intermetallics* **12**, 151 (2004).
- ²⁴ V. K. Pecharsky and K. A. Gschneidner, Jr., *Adv. Mater.* **13**, 683 (2001).
- ²⁵ C. Ritter, C. Magen, L. Morellon, P. A. Algarabel, M. R. Ibarra, V. K. Pecharsky, A. O. Tsokol, and K. A. Gschneidner, Jr., *J. Phys.: Condens. Matter* **18**, 3937 (2006).
- ²⁶ C. Magen, L. Morellon, Z. Arnold, P. A. Algarabel, C. Ritter, M. R. Ibarra, J. Kamarad, A. O. Tsokol, K. A. Gschneidner, Jr., and V. K. Pecharsky, *Phys. Rev. B* **74**, 134427 (2006).
- ²⁷ C. Magen, C. Ritter, L. Morellon, P. A. Algarabel, M. R. Ibarra, A. O. Tsokol, K. A. Gschneidner, Jr., and V. K. Pecharsky, *Phys. Rev. B* **74**, 174413 (2006).
- ²⁸ C. Magen, L. Morellon, P. A. Algarabel, M. R. Ibarra, Z. Arnold, and C. Ritter, *Adv. Solid State Phys.* **46**, 241 (2008).

-
- ²⁹ Z. Arnold, C. Magen, L. Morellon, P. A. Algarabel, J. Kamarad, M. R. Ibarra, V. K. Pecharsky, and K. A. Gschneidner, Jr., *Phys. Rev. B* **79**, 144430 (2009).
- ³⁰ A. O. Pecharsky, K. A. Gschneidner, Jr., V. K. Pecharsky, D. L. Schlagel, and T. A. Lograsso, *Phys. Rev. B* **70**, 144419 (2004).
- ³¹ Ya. Mudryk, V. K. Pecharsky, and K. A. Gschneidner, Jr., *Z. Anorg. Allg. Chem.* **637**, 1948 (2011).
- ³² V. K. Pecharsky, A. P. Holm, K. A. Gschneidner, Jr., and R. Rink, *Phys. Rev. Lett.* **91**, 197204 (2003).
- ³³ J. M. Cadogan, D. H. Ryan, Z. Altounian, X. Liu, and I. P. Swainson, *J. Appl. Phys.* **95**, 7076 (2004).
- ³⁴ D. L. Schlagel, T. A. Lograsso, A. O. Pecharsky, and J. A. Sampaio, *Light Metals 2005 TMS*, 1177 (2005).
- ³⁵ Materials Preparation Center, The Ames Laboratory, U.S. Department of Energy, Ames, IA, USA, www.mpc.ameslab.gov.
- ³⁶ D. X. Chen, E. Pardo, and A. Sanchez, *IEEE Trans. Magn.* **38**, 1742 (2002).
- ³⁷ A. P. Holm, V. K. Pecharsky, K. A. Gschneidner, Jr., R. Rink, and M. N. Jirmanus, *Rev. Sci. Instrum.* **75**, 1081 (2004).
- ³⁸ B. Hunter, Rietica - A visual Rietveld program, International Union of Crystallography Commission on Powder Diffraction Newsletter No. 20, (Summer, 1998) <http://www.rietica.org>.
- ³⁹ M. Zou, Ya. Mudryk, V. K. Pecharsky, K. A. Gschneidner, Jr., D. L. Schlagel, and T. A. Lograsso, *Phys. Rev. B* **75**, 024418 (2007).
- ⁴⁰ R. Nirmala, Ya. Mudryk, V. K. Pecharsky, and K. A. Gschneidner, Jr., *Phys. Rev. B* **76**, 104417 (2007).
- ⁴¹ Ya. Mudryk, Y. Lee, T. Vogt, K. A. Gschneidner, Jr., and V. K. Pecharsky, *Phys. Rev. B* **71**, 174104 (2005).

-
- ⁴² Yu. Mozharivskyj, A. O. Pecharsky, V. K. Pecharsky, and G. J. Miller, *J. Am. Chem. Soc.* **127**, 317 (2005).
- ⁴³ C. Magen, L. Morellon, P. A. Algarabel, M. R. Ibarra, Z. Arnold, J. Kamarad, T. A. Lograsso, D. L. Schlagel, V. K. Pecharsky, A. O. Tsokol, and K. A. Gschneidner, Jr., *Phys. Rev. B* **72**, 024416 (2005).
- ⁴⁴ D. Haskel, Y. B. Lee, B. N. Harmon, Z. Islam, J. C. Lang, G. Srajer, Ya. Mudryk, K. A. Gschneidner, Jr., and V. K. Pecharsky, *Phys. Rev. Lett.* **98**, 247205 (2007).
- ⁴⁵ D. Paudyal, V. K. Pecharsky, K. A. Gschneidner, Jr., and B. N. Harmon, *Phys. Rev. B* **73**, 144406 (2006).
- ⁴⁶ Ya. Mudryk, D. Paudyal, V. K. Pecharsky, and K. A. Gschneidner, Jr., *Phys. Rev. B* **77**, 024408 (2008).
- ⁴⁷ M. Khan, D. Paudyal, Ya. Mudryk, K. A. Gschneidner, Jr., and V. K. Pecharsky, *Phys. Rev. B* **83**, 134437 (2011).

Figure captions:

Fig. 1 (Color online) The x-ray powder diffraction patterns of Er_5Si_4 collected at 300 K (a) and 50 K (b). The upper set of markers indicates positions of Bragg peaks of the orthorhombic phase and the second set of markers indicates positions of Bragg peaks of the monoclinic phase. The two lower sets correspond to minor W peaks (tungsten dendrites are dispersed inside grains during crystal growth; average concentration of W is 2 wt.%), and Cu peaks, which were introduced on the surface during x-ray sample preparation (polishing of the sample embedded in a copper sample holder).

Fig. 2 (Color online) The magnetization of Er_5Si_4 as a function of temperature measured on heating of ZFC (zero field cooled) samples along the three main crystallographic directions: a) along the a -axis; b) along the b -axis; and c) along the c -axis. The fields shown in the plots are applied external magnetic field.

Fig. 3 (Color online) The reciprocal magnetic susceptibility (HM^{-1}) of Er_5Si_4 measured in 1 kOe dc magnetic field applied along main crystallographic directions: a) along the a -axis; b) along the b -axis; and c) along the c -axis. The insets show the thermal hysteresis near the high temperature structural transitions. Solid lines are least squares fits using the Curie-Weiss expression.

Fig. 4 (Color online) The change of the temperature of the structural transition in the paramagnetic Er_5Si_4 with applied magnetic field: a) magnetic field applied along the a -axis; b) magnetic field applied along the b -axis; c) magnetic field applied along the c -axis.

Fig. 5 (Color online) The magnetization of the Er_5Si_4 single crystal measured along the three main crystallographic directions at 5 K as a function of internal magnetic field.

Fig. 6 (Color online) The ac magnetic susceptibility of Er_5Si_4 measured along the three main crystallographic directions. The inset shows an imaginary part of the ac susceptibility.

Fig. 7 (Color online) Change of the concentration of the orthorhombic phase with temperature for Er_5Si_4 between 150 K and 300 K. The results obtained during heating in 40 kOe show no difference with zero field data.

Fig. 8 (Color online) Temperature dependence of lattice parameters and unit cell volumes of both monoclinic (filled circles) and orthorhombic (open squares) Er_5Si_4 phases determined during heating in zero magnetic field. The error bars are smaller or equal to the size of the symbols.

Fig. 9 (Color online) The lattice parameters of Er_5Si_4 in the temperature range from 5 to 50 K during heating in zero magnetic field.

Fig. 10 (Color online) Change of the concentration of the orthorhombic phase with applied magnetic field at 7, 15 and 25 K.

Fig. 11 (Color online) Magnetic field dependence of lattice parameters and unit cell volume of monoclinic Er_5Si_4 at 7 K. The relative changes of the values shown in the figure are for the magnetic field change from 0 to 40 kOe.

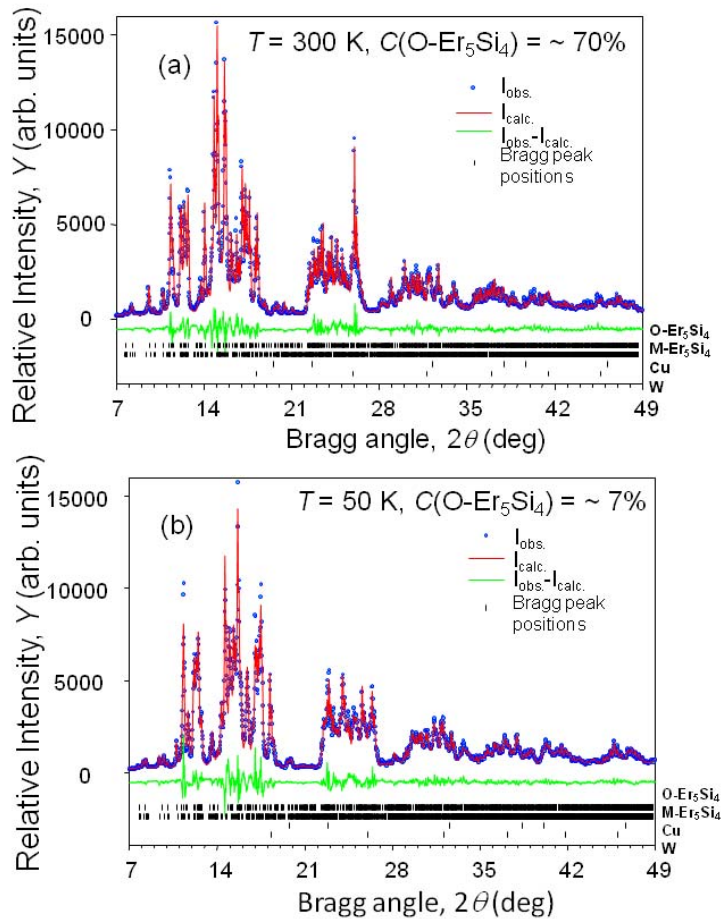


Fig. 1 (Color online) The x-ray powder diffraction patterns of Er_5Si_4 collected at 300 K (a) and 50 K (b). The upper set of markers indicates positions of Bragg peaks of the orthorhombic phase and the second set of markers indicates positions of Bragg peaks of the monoclinic phase. The two lower sets correspond to minor W peaks (tungsten dendrites are dispersed inside grains during crystal growth; average concentration of W is 2 wt.%), and Cu peaks, which were introduced on the surface during x-ray sample preparation (polishing of the sample embedded in a copper sample holder).

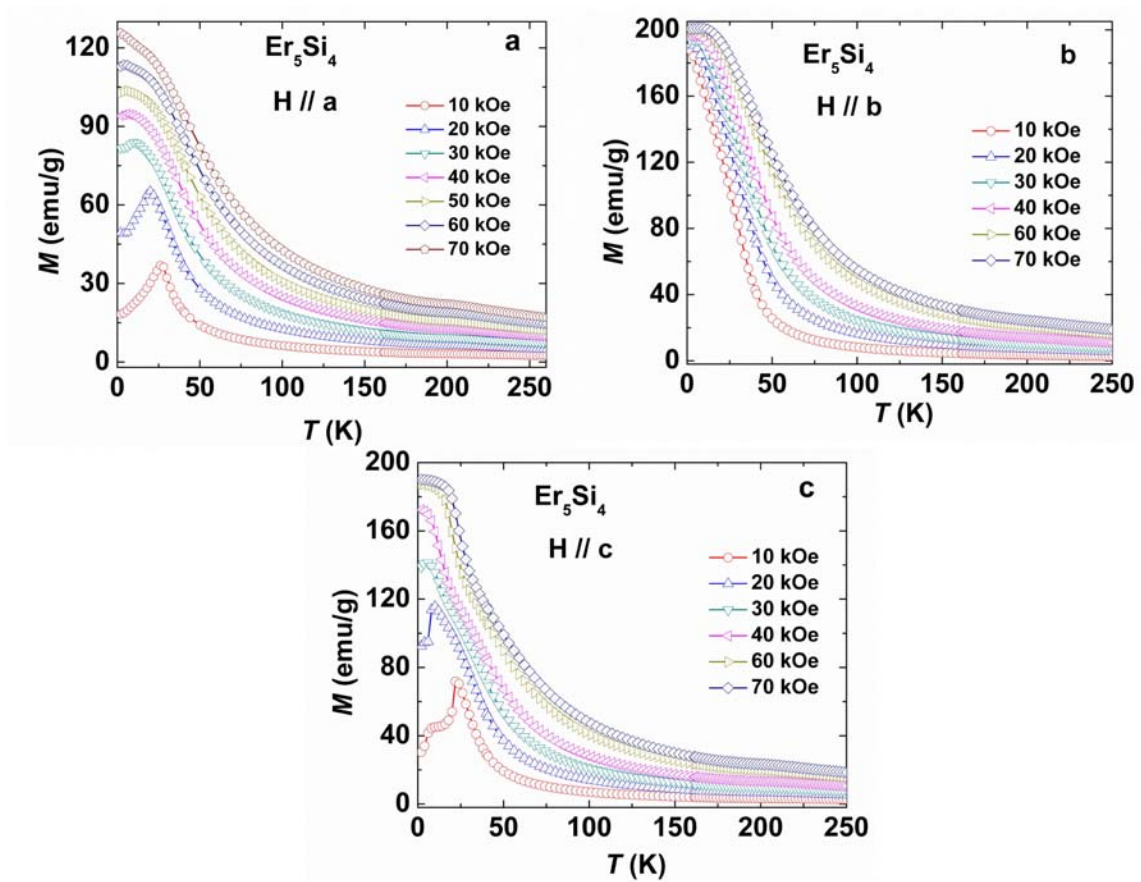


Fig. 2 (Color online) The magnetization of Er_5Si_4 as a function of temperature measured on heating of ZFC (zero field cooled) samples along the three main crystallographic directions: a) along the a -axis; b) along the b -axis; and c) along the c -axis. The fields shown in the plots are applied external magnetic field.

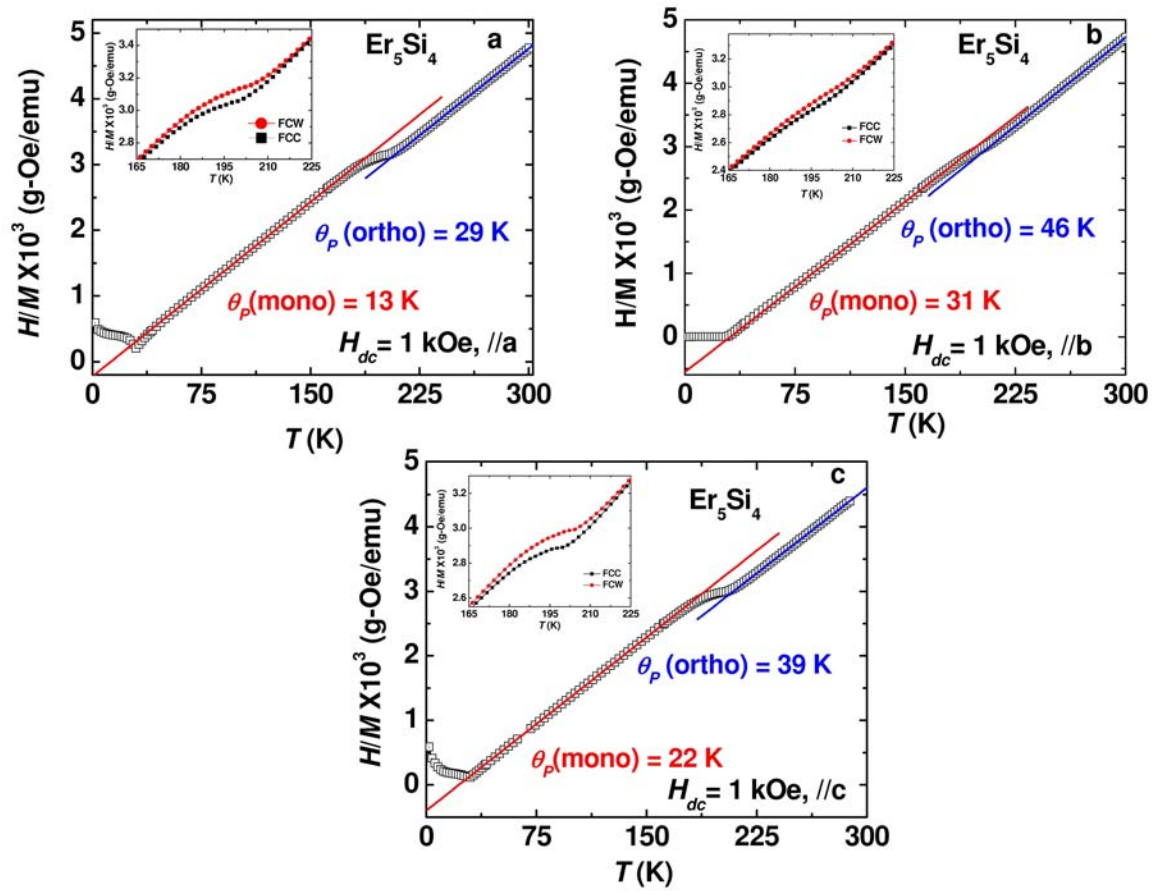


Fig. 3 (Color online) The reciprocal magnetic susceptibility ($H M^{-1}$) of Er_5Si_4 measured in 1 kOe dc magnetic field applied along main crystallographic directions: a) along the a -axis; b) along the b -axis; and c) along the c -axis. The insets show the thermal hysteresis near the high temperature structural transitions. Solid lines are least squares fits using the Curie-Weiss expression.

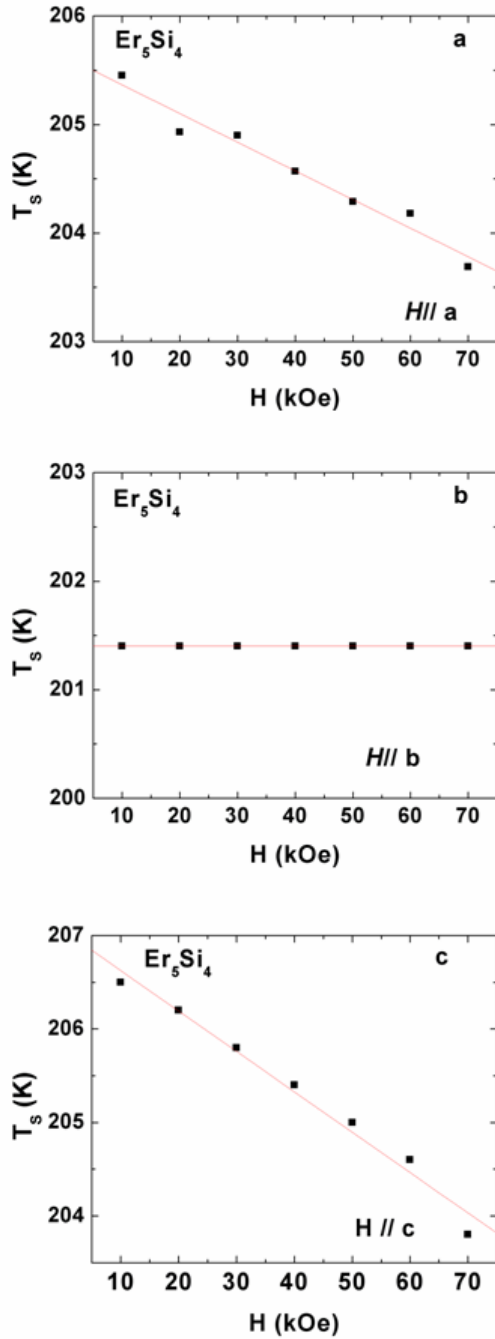


Fig. 4 (Color online) The change of the temperature of the structural transition in the paramagnetic Er_5Si_4 with applied magnetic field: a) magnetic field applied along the a -axis; b) magnetic field applied along the b -axis; c) magnetic field applied along the c -axis.

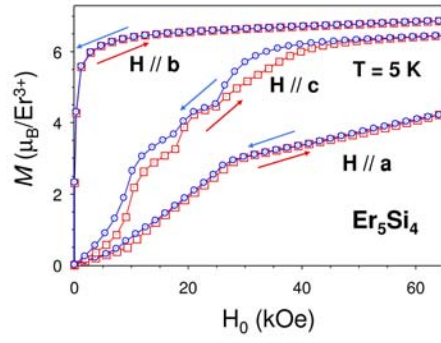


Fig. 5 (Color online) The magnetization of the Er_5Si_4 single crystal measured along the three main crystallographic directions at 5 K as a function of internal magnetic field.

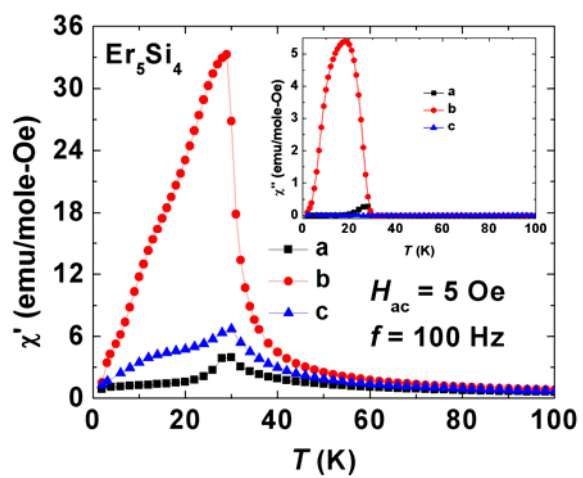


Fig. 6 (Color online) The ac magnetic susceptibility of Er₅Si₄ measured along the three main crystallographic directions. The inset shows an imaginary part of the ac susceptibility.

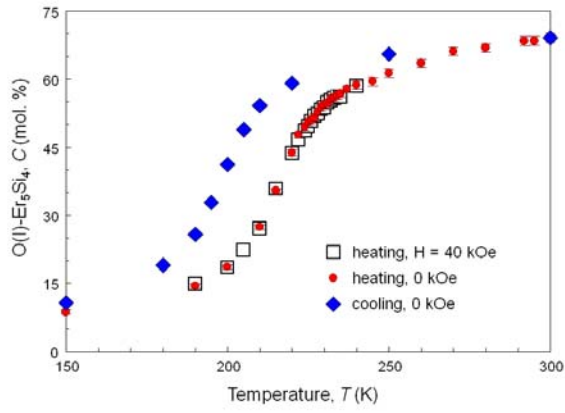


Fig. 7 (Color online) Change of the concentration of the orthorhombic phase with temperature for Er_5Si_4 between 150 K and 300 K. The results obtained during heating in 40 kOe show no difference with zero field data.

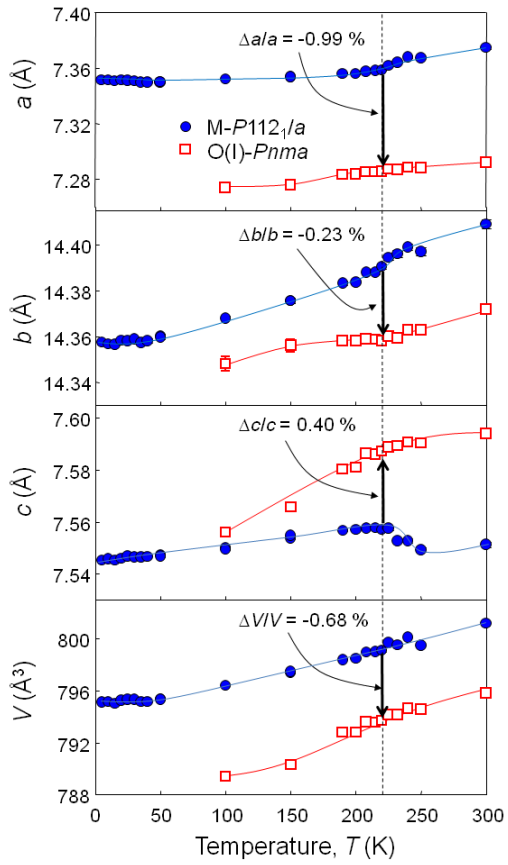


Fig. 8 (Color online) Temperature dependence of lattice parameters and unit cell volumes of both monoclinic (filled circles) and orthorhombic (open squares) Er_5Si_4 phases determined during heating in zero magnetic field. The error bars are smaller or equal to the size of the symbols.

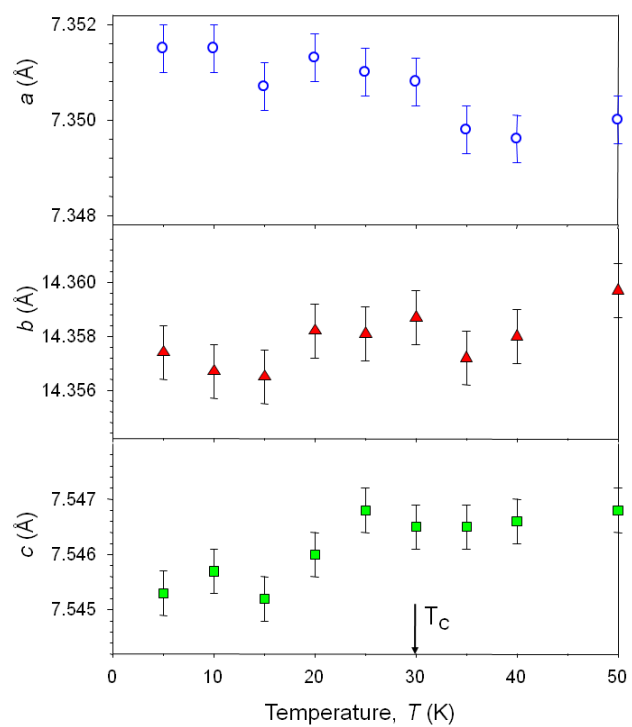


Fig. 9 (Color online) The lattice parameters of Er_5Si_4 in the temperature range from 5 to 50 K during heating in zero magnetic field.

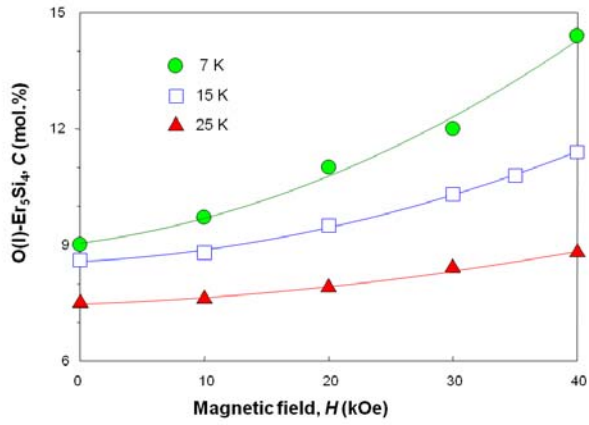


Fig. 10 (Color online) Change of the concentration of the orthorhombic phase with applied magnetic field at 7, 15 and 25 K.

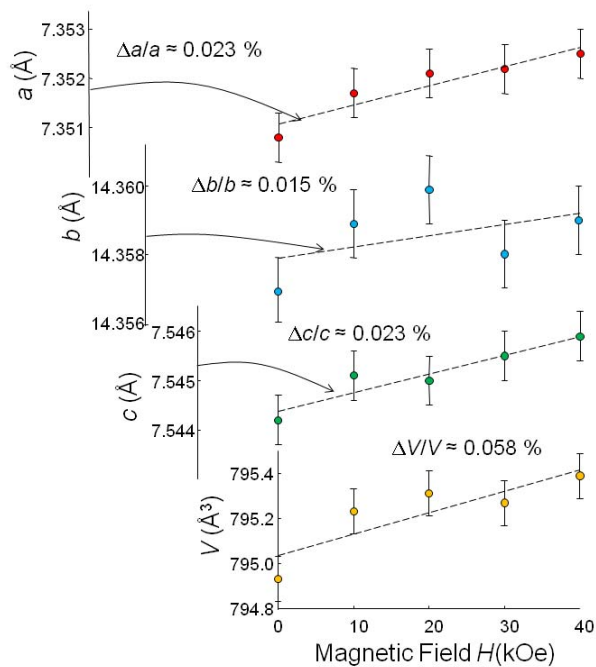


Fig. 11 (Color online) Magnetic field dependence of lattice parameters and unit cell volume of monoclinic Er_5Si_4 at 7 K. The relative changes of the values shown in the figure are for the magnetic field change from 0 to 40 kOe.